

Article

Effects of Engine Load and Ternary Mixture on Combustion and Emissions from a Diesel Engine Using Later Injection Timing

Jun Cong Ge ^{1,*}, Jung Young Kim ², Byeong O Yoo ² and Jun Hee Song ^{2,3,*} 

¹ Division of Mechanical Design Engineering, Jeonbuk National University, 567 Baekje-daero, Deokjin-gu, Jeonju-si 54896, Jeollabuk-do, Republic of Korea

² Graduate School of Industrial Technology, Jeonbuk National University, 567 Baekje-daero, Deokjin-gu, Jeonju-si 54896, Jeollabuk-do, Republic of Korea

³ Department of Convergence Technology Engineering, Jeonbuk National University, 567 Baekje-daero, Deokjin-gu, Jeonju-si 54896, Jeollabuk-do, Republic of Korea

* Correspondence: jcge@jbnu.ac.kr (J.C.G.); sjhee@jbnu.ac.kr (J.H.S.)

Abstract: As a high oxygenated fuel, bioethanol has already obtained more and more widespread attention in diesel engines. The present work aims to study and compare effects of various diesel-bioethanol-biodiesel ternary mixture fuels on combustion and emissions from a four-cylinder diesel engine. A series of engine experiments are conducted on neat diesel fuel (D100), 95% D100 blended with 5% bioethanol and 1% biodiesel by volume (D95E5B1), 90% D100 blended with 10% bioethanol and 1% biodiesel by volume (D90E10B1), and 85% D100 blended with 15% bioethanol and 1% biodiesel by volume (D85E15B1) according to various engine loads (40, 80 and 120 Nm). The experimental results show that the peak value of pressure and heat release rate (HRR) in the cylinder, nitrogen oxides (NO_x) and smoke emissions increase with the increase in engine load, but the brake specific fuel consumption (BSFC) decreases. There is no significant variation in cylinder pressure with the addition of ethanol, but HRR is improved and NO_x and smoke emissions are effectively controlled. It is exciting that the addition of ethanol can simultaneously reduce NO_x and smoke emissions under medium and high load conditions. Specifically, at 120 Nm, ethanol addition simultaneously reduces NO_x emissions by 2.08% and smoke opacity by 36.08% on average. Through the results of this study, it is found that the ethanol can improve the combustion of the four-cylinder diesel engine and also effectively control the emissions of NO_x and smoke. Therefore, ethanol will play an important role in the future research field of energy saving and emission reduction for diesel engines.

Keywords: diesel engine; bioethanol; biodiesel; ternary mixture fuel; later injection



check for updates

Citation: Ge, J.C.; Kim, J.Y.; Yoo, B.O.; Song, J.H. Effects of Engine Load and Ternary Mixture on Combustion and Emissions from a Diesel Engine Using Later Injection Timing. *Sustainability* **2023**, *15*, 1391. <https://doi.org/10.3390/su15021391>

Academic Editor: Antonio Galvagno

Received: 22 November 2022

Revised: 6 January 2023

Accepted: 7 January 2023

Published: 11 January 2023



Copyright: © 2023 by the authors. Licensee MDPI, Basel, Switzerland. This article is an open access article distributed under the terms and conditions of the Creative Commons Attribution (CC BY) license (<https://creativecommons.org/licenses/by/4.0/>).

1. Introduction

Based on high thermal efficiency, output power, stability and low fuel consumption, diesel engines are widely used in passenger vehicle, truck, ships, construction and agricultural machinery, and other fields. However, the disadvantage of diesel engines is that they emit more nitrogen oxides (NO_x) and smoke emissions than gasoline engines due to the fuel/air mixing-controlled combustion [1,2]. Although electric vehicles (EVs) do not produce any emissions during driving, if the generation process of electricity relies too much on fossil fuels, it also emits carbon dioxide (CO₂) and other harmful emissions in the life cycle assessment (LCA). According to the global car sales report released by the International Energy Agency (IEA), the ownership of EVs only accounted for 8.57% of total global car ownership in 2021—that is, the internal combustion engine (ICE) still occupied the dominant position. However, as these regulations become stricter with respect to emissions, improving combustion efficiency and reducing emissions has become the main development direction of ICE. Therefore, how to effectively reduce the above harmful emissions is of great significance in promoting the green and healthy development of diesel engines.

At present, many researchers have proposed the following effective methods to reduce diesel engine emissions, including variable valve timing (VVT) strategy, variable compression ratio (VCR) strategy, exhaust aftertreatment system, new combustion technology, biofuel, and multiple-injection strategies. Xu et al. [2] reported that the combustion process of a diesel engine can be effectively controlled by optimizing VVT and VCR strategies, so as to achieve the goal of highly efficient combustion and low emissions in diesel engines. In addition, the optimization of VVT strategy is conducive to improving the exhaust gas temperature to ensure the efficient operation of the catalyst in the exhaust aftertreatment systems [3]. However, the application of VVT sometimes leads to negative effects such as increased fuel consumption. Honardar et al. [4] pointed out that the brake specific fuel consumption (BSFC) increases by nearly 11% with VVT operation. On the other hand, at present, the method of reducing diesel engine exhaust emissions is mainly realized through the exhaust aftertreatment devices (i.e., DOC, DPF, SCR, EGR). The function of diesel oxidation catalyst (DOC) is to catalyze CO and HC emitted by diesel engines to form CO₂ and water. A diesel particulate filter (DPF) is a device to effectively capture diesel soot particles, and selective catalytic reduction (SCR) and exhaust gas recirculation (EGR) are devices to effectively reduce diesel NO_x emissions. However, these devices all have different disadvantages. For example, DOC has a strong dependence on exhaust temperature. Generally, most catalysts require exhaust gas temperature between 250 and 400 °C [3]. It is difficult for catalysts to work at low temperatures. Moreover, the conventional catalysts of DOC are mainly transition metals and noble metal groups such as Pt, Pd and Rh, and the use of these metals will lead to higher costs [5]. During the use of DPF, filter blockage often occurs, which leads to the increase in engine back pressure and the decrease in combustion efficiency. This requires a method to burn the accumulated particles regularly, which is called regeneration, including active regeneration and passive regeneration [6]. Active regeneration has high requirements for exhaust temperature. Active regeneration can only be carried out when the temperature exceeds 550 °C, but often at the expense of higher fuel consumption [7]. Although passive regeneration is not limited by temperature, it needs to add fuel additives or catalysts to reduce the ignition temperature of particles, but excessive additives will affect the life of DOC [8]. On the other hand, NO_x reduction through SCR often requires the addition of urea. This is because urea generates NH₃ after hydrolysis and pyrolysis at high temperature, and NO_x is reduced to N₂ by NH₃ on the surface of SCR system catalyst [9,10]. The working principle of EGR mainly depends on recovering part of exhaust gas into the cylinder to reduce the maximum combustion temperature by reducing the amount of fresh air, so as to curb excessive NO_x generation. However, its disadvantages are low combustion efficiency and high fuel consumption [11]. Therefore, compared with these methods, developing alternative fuels such as biodiesel and bioethanol is the simplest and most effective way to reduce the harmful emissions from diesel engines.

Biodiesel can be regarded as the ideal alternative fuel for diesel engines, because it has a high cetane number with better ignition characteristics [12,13]. Higher oxygen content can promote the complete combustion of the fuel. In addition, biodiesel can be mixed with diesel fuel in any proportion based on the fact its fuel properties are very similar to diesel fuel [14–16]. Zhang et al. [5] investigated diesel and biodiesel on emission and combustion characteristics of a four-cylinder diesel engine. They found that adding biodiesel resulted in an average reduction of 35%, 64% and 45% in CO, HC and smoke, respectively. However, the experimental results show that the addition of biodiesel leads to more CO emissions than diesel because the higher viscosity of biodiesel is not conducive to atomization [17]. Therefore, some researchers tried to use alcohols (e.g., ethanol, methanol) to mix biodiesel and diesel and studied the effects of these ternary mixed fuels on diesel engine combustion and emission characteristics [18,19]. Kwanchareon et al. [20] pointed out that 80% diesel fuel mixed with 5% ethanol and 15% biodiesel is the best mixing ratio considering the fuel properties and the effect on emission reduction. Noorollahi et al. [21] tested various diesel–biodiesel–ethanol blends on a single diesel engine. However, the above literature review shows there is a lack of research on the following points: (i) most

researchers use a single-cylinder diesel engine as the main object; (ii) different engines lead to inconsistent experimental results; and (iii) there are few studies that focus on ethanol, and many previous studies have focused on nano additives, such as alumina nano additives, in diesel-biodiesel-ethanol blends. Therefore, in view of the research gaps in the previous studies, it is necessary to directly investigate the influences of various diesel-biodiesel-ethanol blends on combustion and emissions of a four-cylinder diesel engine. In addition, ethanol was the main experimental variable in this study. As much as 15 vol.% ethanol was added to the mixture of diesel and biodiesel. No other additives was used.

To investigate the improvement effect of bioethanol on combustion and emissions in a four-cylinder common rail direct injection (CRDI) diesel engine, especially for control of NO_x and smoke emissions, a series of engine tests were carried out. Four tested fuels including neat diesel fuel (D100), 95% D100 blended with 5% ethanol and 1% biodiesel (D95E5B1), 90% D100 blended with 10% ethanol and 1% biodiesel (D90E10B1), and 85% D100 blended with 15% ethanol and 1% biodiesel (D85E15B1) were prepared and tested in the diesel engine. All fuels were mixed according to the volume ratio. The experimental results show that adding a proper amount of bioethanol to diesel can simultaneously reduce NO_x and smoke emissions under medium and high load conditions. Therefore, it can be expected that bioethanol is likely to be widely used in diesel engines as a fuel additive in the future to control NO_x and smoke emissions.

2. Materials and Methods

2.1. Engine and Fuel

Figure 1 displays the representation of the experimental setup. Specifications of the engine are shown in Table 1. Four tested fuels were prepared for engine testing: neat diesel fuel (D100), 95% D100 blended with 5% ethanol and 1% biodiesel (D95E5B1), 90% D100 blended with 10% ethanol and 1% biodiesel (D90E10B1), and 85% D100 blended with 15% ethanol and 1% biodiesel (D85E15B1). The main fuel properties are listed in Table 2.

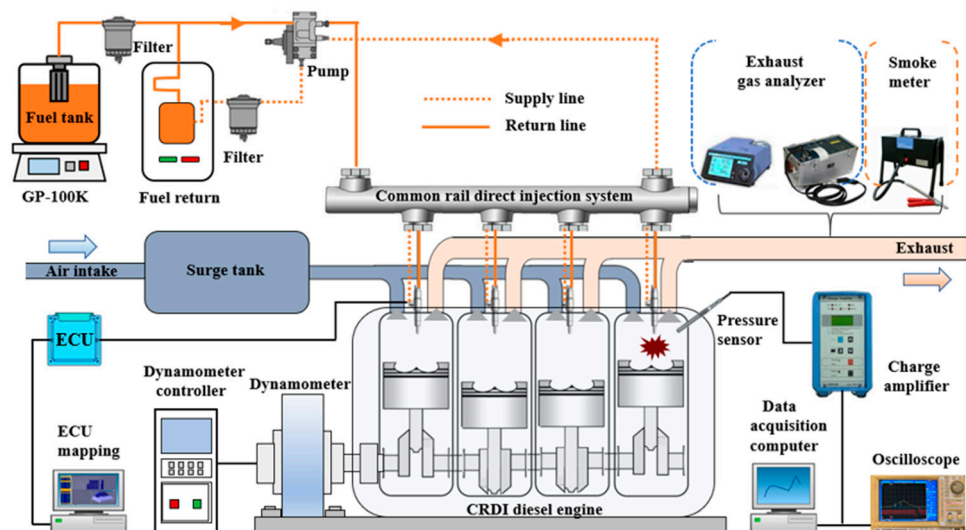


Figure 1. Experimental apparatus.

Table 1. Specifications of the four-cylinder diesel engine.

Engine Parameter	Specifications
Engine type	In-line 4-cylinder
Cooling system	Water cooling
Air intake system	Turbocharger with WGT
Number of cylinders	4
Bore × stroke	83 × 92 (mm)
Injector hole diameter	0.17 (mm)
Number of injector nozzle holes	5
Injector spray angle	150 (degree)
Compression ratio	17.7:1
Max. power	82/4000 (kW/rpm)

Table 2. Properties of diesel, ethanol and biodiesel.

Properties (Units)	Diesel Fuel	Bioethanol	Biodiesel	Test Method
Density (kg/m ³ @ 15 °C)	836.8	799.4	877	ASTM D941
Viscosity (mm ² /s @ 40 °C)	2.719	1.10	4.56	ASTM D445
Calorific value (MJ/kg)	43.96	28.18	39.72	ASTM D4809
Cetane index	55.8	8	57.3	ASTM D4737
Flash point (°C)	55	12	196	ASTM D93
Oxygen content (%)	0	34.7	11.26	-

2.2. Experimental Conditions and Measurements

Experiments were performed on the CRDI diesel engine according to three engine loads (40, 80, 120 Nm) with a constant engine speed of 1800 rpm. The pilot/main injection timing and injection pressure were respectively controlled at 5/10 °CA ATDC and 50 MPa. Table 3 lists the main experimental conditions. Table 4 shows the range, resolution and uncertainty of relevant test equipment. The engine speed and load were controlled by a DYTEK230 dynamometer. The fuel consumption in the experiment was measured by a GP-100K weighing balance. As the most important value for analyzing combustion characteristics, the in-cylinder pressure was measured by a 6056A Kistler pressure sensor with a charge amplifier. The pressure data in the cylinders were recorded over 200 consecutive engine cycles. For the measurement of engine exhaust emissions, a Horiba exhaust gas analyzer (MEXA-554JK, Horiba, Kyoto, Japan) was employed to measure the HC and NO_x emissions, and a multiple gas analyzer (GreenLine MK2, Eurotron [Korea] Ltd., Seoul, Korea) was employed to measure the CO emissions. An OP-160 smokemeter was employed to measure smoke opacity. Based on the variability of the engine, all experimental data were recorded after the engine ran stably—that is, the temperature of cooling water reached 85 °C.

Table 3. Experimental conditions.

Item	Conditions
Fuel	D100, D95E5B1, D90E10B1, D85E15B1
Load	40, 80, 120 Nm
Speed	1800 rpm
Injection pressure	50 MPa
Pilot/main injection timing	5/10° ATDC
Intake air temperature	25 ± 1 °C
Cooling water temperature	85 ± 1 °C

Table 4. The rang, resolution and uncertainty of experimental equipment.

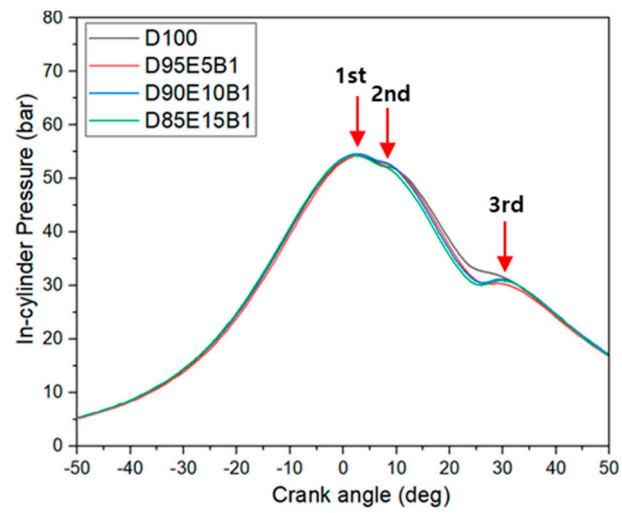
Device	Range	Resolution	Uncertainty
CO (ppm)	0–4000	1	±0.62%
HC (ppm)	0–10,000	1	±5%
NOx (ppm)	0–6000	1	±0.25%
Smoke opacity (%)	0–100	0.1	±1%
Engine load (Nm)	0–833	0.1	±0.2%
Engine speed (rpm)	0–10,000	1	±0.1
Fuel consumption (g)	0–101	1	±1.98
In-cylinder pressure (bar)	0–250	0.1	±0.01

3. Experimental Results and Discussion

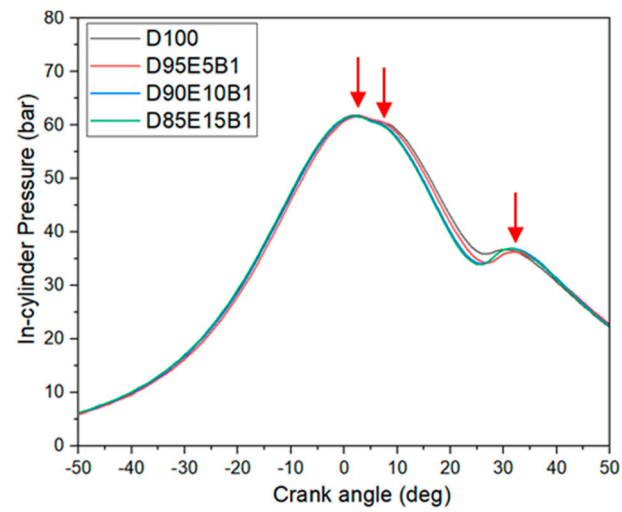
3.1. Combustion Characteristics

3.1.1. Pressure in the Cylinder

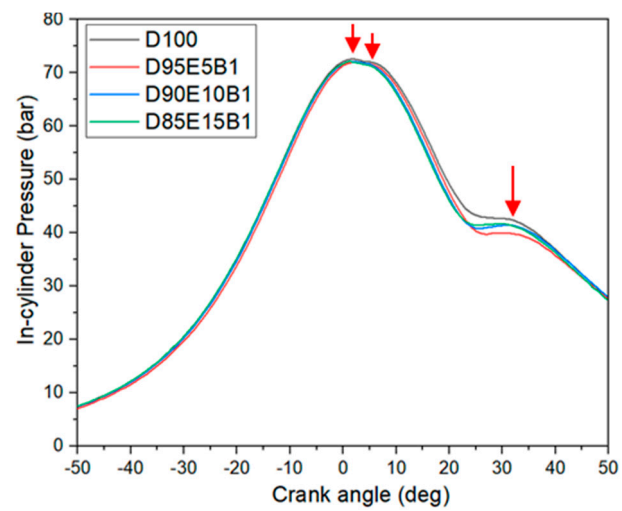
Figure 2 shows the in-cylinder pressures of four test fuels according to different engine loads under a constant engine speed of 1800 rpm. Generally, for diesel engines with pilot and main injection strategy, the pressure curve in the cylinder has two peaks, which are caused by pilot and main injection, respectively [22]. When the main injection timing occurs before top dead center (BTDC), the peak value of in-cylinder pressure of main injection is greater than that of pilot injection. However, when the main injection occurs after top dead center (ATDC), the maximum pressure caused by the main injection is smaller than that of the pilot injection [23]. In this study, the pilot and injection timing occurred at ATDC 5° and 10°, respectively. Therefore, the pressure peak caused by main injection is far lower than that of pilot injection. This is because the piston is already in the process of moving from top dead center (TDC) to bottom dead center (BDC), and the cylinder volume gradually increases to offset some of the pressure caused by fuel combustion. In addition, as shown in Figure 2, three pressure peaks can be clearly observed, appearing at the TDC, the ATDC 5° and 10°, respectively. The first pressure peak may be related to the pressure generated by the piston in the compression process and some residual heat generated by the later fuel combustion. The second and third pressure peaks are caused by pilot and main injection fuel combustion, respectively. The reason the third pressure peak is much lower than the first and second is that combustion occurs far away from the TDC during the expansion stroke [24]. Therefore, as shown in Figure 2, under the same load, the maximum value of in-cylinder values for all fuels are almost the same. These results are not quite the same as those reported by Sittichompoo et al. [25]. They investigated the combustion and emissions of a single-cylinder diesel engine fueled with different diesel-biodiesel-ethanol blends (E0, E10, E20, E30, E40, E50). They pointed out that the addition of ethanol would significantly delay the start of ignition, and when a large amount of ethanol was added to the blended fuel, the maximum in-cylinder pressure was far lower than that of diesel. This may be because the diesel engine in this study is a four-cylinder engine, and the combustion characteristics variation is more complex than that of a single-cylinder engine. In addition, the difference from [25] is that no other additives, including hydrogen, are added in this study. On the other hand, for most fuels, the maximum value of in-cylinder values occurs at ATDC 3° under low load (40 Nm) conditions, and it occurs at ATDC 2° under medium (80 Nm) and high load (120 Nm) conditions. The reason the maximum pressure occurs earlier on the crankshaft angle may be related to the large amount of residual heat generated under medium and high load conditions.



(a) 40 Nm



(b) 80 Nm



(c) 120 Nm

Figure 2. In-cylinder pressure.

Figure 3 shows the maximum in-cylinder pressures of four test fuels under different engine loads. Generally speaking, the addition of biodiesel and alcohol fuel will lead to higher maximum pressure in the cylinder than that of diesel fuel. Because biodiesel and alcohol fuel are both oxygenated fuels, the presence of oxygen will improve combustion to a certain extent [26]. In addition, the cylinder pressure is also directly related to fuel viscosity, cetane number and other properties. Fuel with low viscosity and high cetane number can form a more uniform mixture when mixed with air, which is beneficial to increasing the in-cylinder pressure [27]. However, as shown in Figure 3, there is no significant variation in the maximum in-cylinder pressure of all test fuels under the same engine load conditions with the addition of ethanol. At 40 Nm, the maximum in-cylinder pressures of D100, D95E5B1, D90E10B1 and D85E15B1 are 54.3 bar, 54.3 bar, 54.6 bar and 54.3 bar, respectively. At 80 Nm, the maximum in-cylinder pressures of D100, D95E5B1, D90E10B1 and D85E15B1 are 61.9 bar, 61.6 bar, 61.6 bar and 61.7 bar, respectively. At 120 Nm, the maximum in-cylinder pressures of D100, D95E5B1, D90E10B1 and D85E15B1 are 72.6 bar, 72.0 bar, 72.1 bar and 72.1 bar, respectively. As mentioned above, the maximum in-cylinder pressure of almost all fuels appears at ATDC 2–3°. At this time, neither pilot injection nor main injection occurs, so the pressure in the cylinder may be mainly attributed to the waste heat generated after the compression of the piston and the combustion of the mixture. Moreover, the maximum in-cylinder pressure shows a gradually increasing trend with the increase in engine load, which is mainly caused by a large amount of fuel being burned under high load. Similar reports were presented by [28,29].

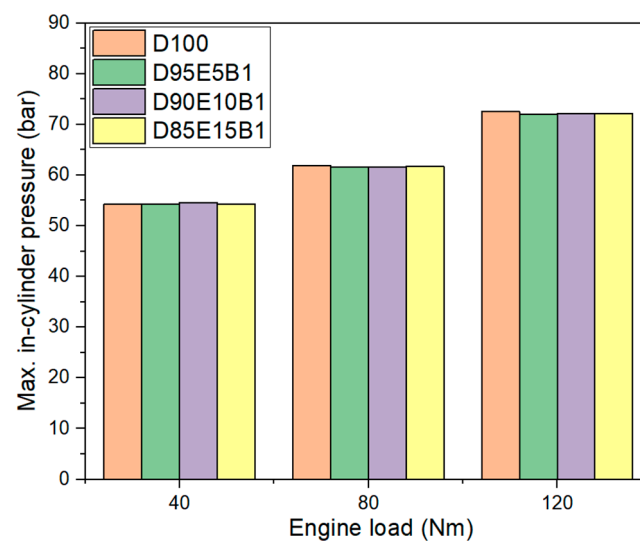
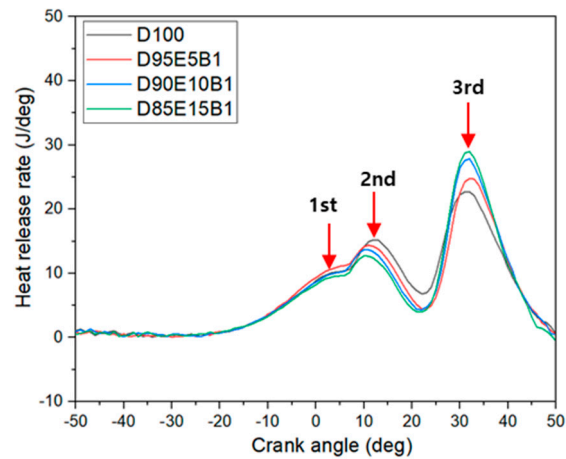


Figure 3. Maximum in-cylinder pressure.

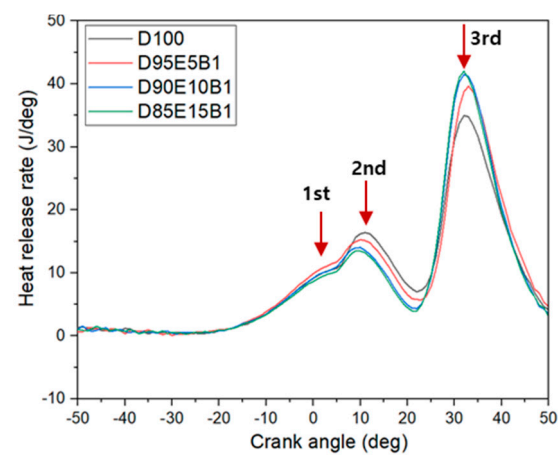
3.1.2. Heat Release Rate in the Cylinder

Figure 4 illustrates the variation of heat release rate (HRR) of four test fuels under different engine load conditions. As shown in Figure 4, similar to the in-cylinder pressure curve, the HRRs of all test fuels have three different peaks, which are respectively caused by piston compression and residual heat, pilot injection, and main injection. The HRR curves of all the test fuels show a similar trend consisting of premixed combustion phase and diffusion combustion phase. Because the pilot injection occurs near the TDC, the temperature and pressure in the cylinder are very high, which causes the fuel to be burned soon after injection—that is, it is difficult to calculate the ignition delay. However, the only thing that can be seen is that the start of combustion (SOC) of D95E5B1 is slightly earlier than that of D100. This may contribute to the improvement of combustion characteristics due to the higher cetane number of biodiesel. However, the SOC of D90E10B1 and D85E15B1 is similar to that of D100, which may be due to the negative effect (increased ignition delay) caused by the low cetane number of bioethanol, which offset the positive effect (shortened

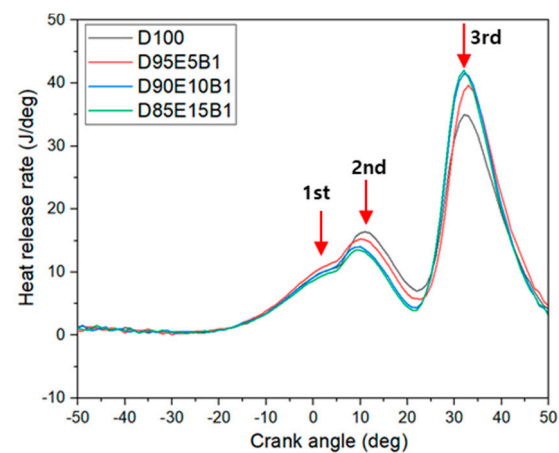
ignition delay) of biodiesel [24]. In addition, after the main injection, the peak value of HHR for all blended fuels are higher than those of diesel. This may be due to the high evaporation latent heat characteristic of ethanol during atomization, which leads to the decrease in ambient pressure and temperature in the cylinder, thus prolonging the ignition delay period and combustion stage of the blended fuel [30].



(a) 40 Nm



(b) 80 Nm



(c) 120 Nm

Figure 4. Heat release rate.

Figure 5 shows the variation of maximum heat release rate (HRR) of four test fuels under different engine load conditions. At 40 Nm, the maximum HRR of D100, D95E5B1, D90E10B1 and D85E15B1 are 22.69, 24.76, 27.85 and 28.96 J/CA, respectively. At 80 Nm, the maximum HRR of D100, D95E5B1, D90E10B1 and D85E15B1 are 34.96, 39.62, 41.50 and 42.00 J/CA, respectively. At 120 Nm, the maximum HRR of D100, D95E5B1, D90E10B1 and D85E15B1 are 38.96, 38.51, 41.04 and 39.23 J/CA, respectively. At low (40 Nm) and medium (80 Nm) load, the maximum HRR of all test fuels increases gradually with the increase in ethanol mixing ratio. At high load (120 Nm), there is no dramatic change in maximum HRR with increase in bioethanol. The above reasons can be summarized as follows [24,26,28,29,31]: (i) low cetane number of ethanol increases the ignition delay, which is conducive to full mixing of fuel and air; (ii) high evaporation latent heat of ethanol leads to the absorption of a large amount of heat around the fuel during atomization, which also increases the ignition delay; (iii) high volatility and low viscosity of ethanol result in it being easy to mix with air, making it easier to form a uniform mixture; (iv) the small droplet size of ethanol increases the spray cone angle and promotes the development of spray, thus improving the air-fuel mixture to promote combustion; (v) high load cause more fuel to be burned and generates a lot of heat, which counteracts the characteristic that ethanol increases ignition delay, so the maximum HRR has no obvious change.

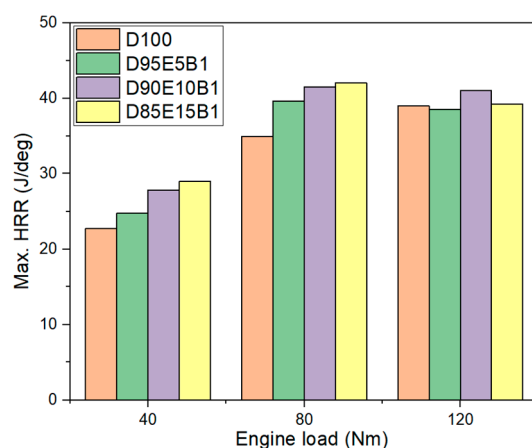


Figure 5. Maximum heat release rate.

3.1.3. Brake Specific Fuel Consumption

Figure 6 shows the variation of brake specific fuel consumption (BSFC) of four test fuels under different engine load conditions. With the increase in engine load, the BSFC of all fuels shows a decreasing trend. Compared with the BSFC at 40 Nm, the BSFC at 80 and 120 Nm are reduced by an average of 18.30% and 18.50%, respectively. This may be attributed to the lower combustion efficiency of the engine due to the relatively low temperature and pressure in the cylinder at a lower load of 40 Nm. In addition, under medium and high load, the temperature and pressure in the cylinder are improved, resulting in slight changes in BSFC. Moreover, the high level of oxygen in ethanol can be fully demonstrated under high engine load to promote complete combustion and reduce fuel consumption. Similar results were obtained in studies by [26,32]. Under the same load, the BSFC of blended fuel shows a gradual increase trend with the increase in bioethanol mixing ratio. At 40 Nm, the BSFC of D95E5B1, D90E10B1 and D85E15B1 are respectively increased by 1.52%, 2.81% and 3.30% compared with D100. At 80 Nm, the BSFC of D95E5B1, D90E10B1 and D85E15B1 are respectively increased by 3.04%, 6.00% and 6.57% compared with D100. At 120 Nm, the BSFC of D95E5B1, D90E10B1 and D85E15B1 are respectively increased by 3.78%, 3.79% and 5.04% compared with D100. The reason for the increase in BSFC with the addition of ethanol is that ethanol has a lower calorific value than diesel, so it needs to burn more fuel to achieve the same power with diesel [26].

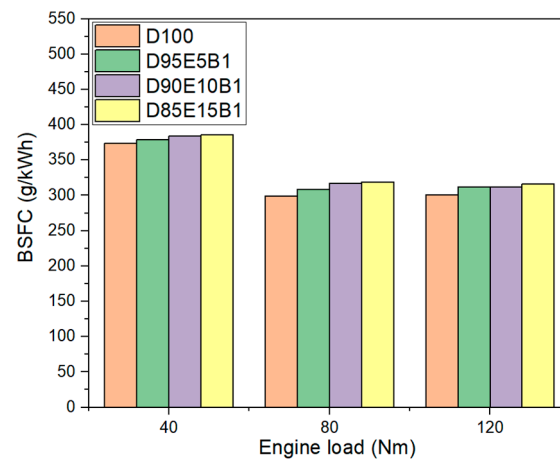


Figure 6. Brake specific fuel consumption.

3.2. Emission Characteristics

3.2.1. Carbon Monoxide

Figure 7 shows the carbon monoxide (CO) emissions for all test fuels according to various engine loads. On the whole, CO emissions decrease first and then increase with the increase in engine load. Compared with 40 Nm, CO emissions decrease by an average of 30.03% at 80 Nm, while they increase by an average of 15.86% at 120 Nm. The CO of all test fuels under medium load is the lowest, which can be attributed to the fact that the fuel and air are mixed evenly, and the combustion conditions such as temperature and pressure are relatively moderate in the cylinder, resulting in more sufficient combustion. However, combustion conditions under low load, such as low cylinder temperature and pressure, are not conducive to complete combustion of fuel. In addition, under the high load of 120 Nm, although the higher temperature and pressure in the cylinder are conducive to combustion, more fuel is injected into the combustion chamber under high load, which causes uneven mixing of fuel and air and incomplete combustion. On the other hand, under the medium and low load, the CO emissions of blended fuels are higher than that of pure diesel fuel, but the opposite result appears under the high load of 120 Nm. This may be because the high evaporation latent heat of ethanol dominates under medium and low load, while the high temperature of the engine under high load counteracts the negative impact of the evaporation latent heat of ethanol, and the oxygen contained in bioethanol promotes fuel combustion more fully, thus reducing the generation of CO emissions. Tutak et al. [33] also pointed out that low temperature and high local equivalence ratio directly affect CO emissions.

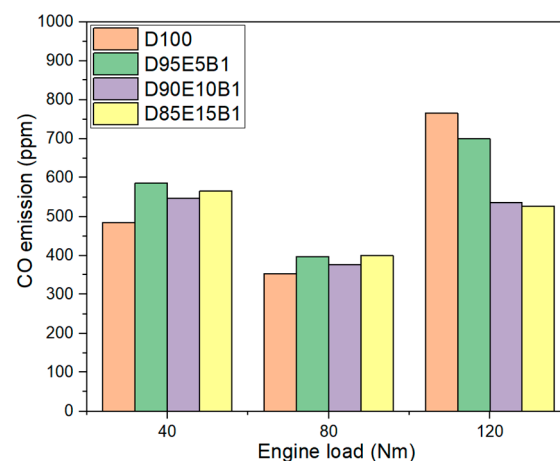


Figure 7. CO emissions.

3.2.2. Hydrocarbon

Figure 8 displays the hydrocarbon (HC) emissions of four test fuels under different engine load conditions. As shown in Figure 8, HC emissions show a gradual decrease trend with the increase in engine load. Compared with HC emissions at 40 Nm, HC emissions of four test fuels at 80 and 120 Nm are averagely decreased by 33.33 and 48.49%, respectively. This is mainly because increasing the engine load increases the temperature in the cylinder, promotes the oxidation of HC, and reduces the probability of misfire, as well as unburned or partial combustion caused by low temperature of the cylinder wall. Similar results were reported by [26,28]. On the other hand, when 5 vol.% of ethanol is added to diesel fuel, HC is shown to be the lowest compared to other test fuels under all test conditions. Under the engine load of 40 Nm, 80 Nm and 120 Nm, the HC of D95E5B1 is respectively reduced by 12.5%, 50.0% and 40.0% compared with that of D100. However, when the mixing ratio of ethanol exceeds 5 vol.%, especially when 15 vol.% of ethanol is added to diesel fuel, HC is respectively increased by 25.0% and 16.67% at 40 Nm and 80 Nm compared with diesel fuel. This may be because after excessive ethanol is added to the diesel fuel, the high evaporation latent heat (cooling effect) of ethanol dominates—that is, the cooling effect is significant—which reduces the temperature in the cylinder and hinders the oxidation of HC emissions [26].

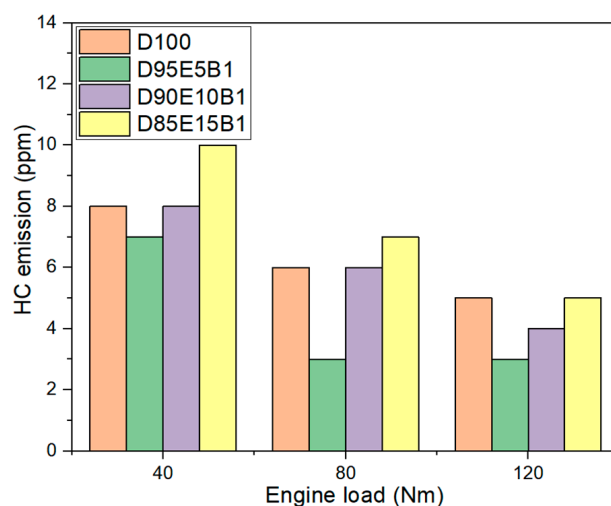


Figure 8. HC emissions.

3.2.3. Nitrogen Oxide

Figure 9 displays the nitrogen oxide (NO_x) emissions of four test fuels under different engine load conditions. NO_x emissions emitted from diesel engines mainly include nitric oxide (NO) and nitrogen dioxide (NO₂), of which the content of NO is the highest, accounting for about 90% [34]. The formation mechanism of NO depends on the combination of some molecular species and some differences in certain fuel properties [35]. As shown in Figure 9, the NO_x emissions of four test fuels shows a gradual increase trend with the increase in engine load. Compared with 40 Nm, NO_x emissions at 80 and 120 Nm are averagely increased by 83.30 and 130.19%, respectively. The formation of NO_x emissions from diesel engines is highly dependent on temperature in the cylinder, local oxygen concentration, and duration of combustion in the high temperature zone [28]. The increase in NO_x caused by the increase in load may be mainly related to more fuel participates in combustion, thus increasing the combustion temperature and combustion duration in the cylinder. Other researchers have reported similar results [36]. In addition to the obvious influence of engine operating conditions on the formation of NO_x, the addition of ethanol also changes the formation of NO_x emissions. Compared with diesel fuel, the ternary mixture fuels give slightly higher NO_x emissions at low engine load of 40 Nm, while they show lower NO_x emissions at medium and high engine loads. At 40 Nm, the NO_x

emissions of D95E5B1, D90E10B1 and D85E15B1 are respectively reduced by 5.37, 21.46 and 28.78% compared with D100. At 80 Nm, the NO_x emissions of D95E5B1, D90E10B1 and D85E15B1 are respectively increased by 5.59, 7.83 and 3.58% compared with D100. At 120 Nm, the NO_x emissions of D95E5B1, D90E10B1 and D85E15B1 are respectively increased by 1.10, 2.56 and 2.56% compared with D100. Because the fuel injected into the cylinder is relatively small under low load condition compared with that under medium and high load conditions. Therefore, compared with the cooling effect of ethanol, the role of high oxygen content plays a leading role, promoting combustion and increasing combustion temperature. However, a great quantity of fuel is injected into the combustion chamber as the load increases, so the cooling effect of ethanol plays a major role in reducing the maximum combustion temperature in the combustion chamber, thereby reducing the NO_x formation.

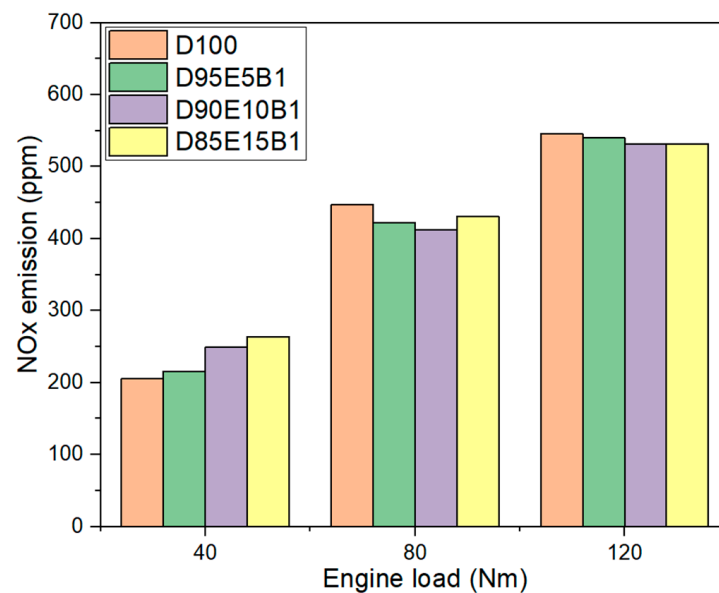


Figure 9. NO_x emissions.

3.2.4. Smoke Opacity

Figure 10 displays the smoke opacity in percentage of four test fuels under different load conditions. Diesel particulate matter (DPM) is mainly composed of soot and some hydrocarbons (soluble organic fraction, SOF) adsorbed on the soot surface. Among the components of DPM, soot is considered to be the main substance that affects the smoke opacity. When there is insufficient air or oxygen in the combustion chamber, the air-fuel ratio will decrease, resulting in a large number of soot particles generated from the thermal decomposition of long-chain molecules [37]. As shown in Figure 10, it can be observed that the smoke opacity shows a gradual increase trend with increase in engine load. Compared with 40 Nm, the smoke opacity at 80 and 120 Nm are averagely increased by 59.57 and 427.66%, respectively. The increase in smoke opacity caused by the increase in load can be explained as the increase in the content of fuel injected into the cylinder, thus reducing the air-fuel ratio, resulting in more fuel-rich areas and incomplete combustion. Other researchers also reported that the increasing of engine load increases the smoke opacity [38]. On the other hand, on the whole, the addition of bioethanol reduces smoke opacity compared with diesel under most conditions. Especially under the high load condition of 120 Nm, there is a significant reduction of smoke opacity with the addition of bioethanol. At 120 Nm, compared with D100, the smoke opacities of D95E5B1, D90E10B1 and D85E15B1 are reduced by 23.53, 40.00 and 44.71%, respectively. This may be related to the addition of ethanol. Firstly, ethanol is a highly oxygenated fuel, and the oxygen can improve the problem of local oxygen deficiency. Secondly, the high volatility and high

latent heat of evaporation of ethanol lead to an increase of the ignition delay, resulting in sufficient mixing time for fuel and air, which is conducive to complete combustion. The low carbon/hydrogen ratio and R-OH group of ethanol, as well as the reduction of the carbon chain length of the blended fuel with the addition of ethanol, are additional major reasons for reducing particle formation [26]. Hulwan et al. [37] also pointed out that the presence of atomic-bound oxygen in ethanol is beneficial to reducing the particles. Moreover, the good volatility of ethanol is conducive to better atomization and vaporization of the mixture, which can reduce the soot generation in the fuel-dense area within the mixed diffusion flame sheath.

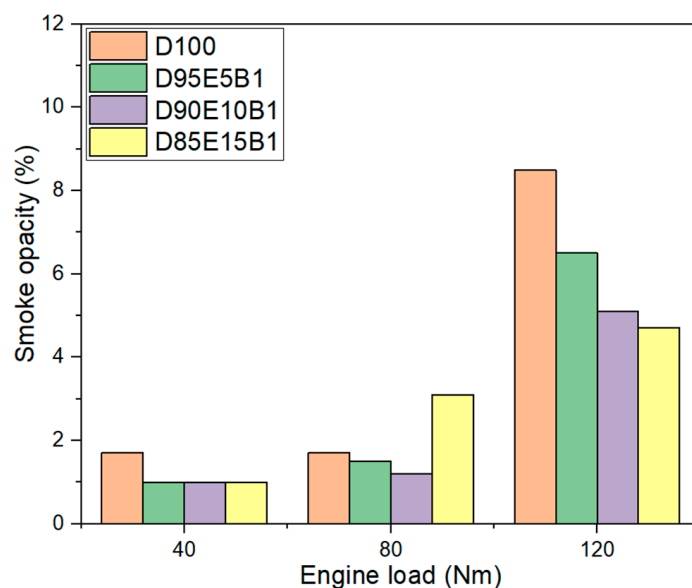


Figure 10. Smoke opacity of all test fuels at different engine loads.

4. Conclusions

In this work, the influences of the diesel-bioethanol-biodiesel ternary mixed fuel on the combustion and emission from a four-cylinder diesel engine were investigated. Four test fuels (D100, D95E5B1, D90E10B1 and D85E15B1) and three engine loads (40, 80 and 120 Nm) were selected as the main experimental variable, and other parameters such as injection pressure and engine speed were controlled at 500 bar and 1800 rpm, respectively. The main conclusions can be summarized as follows:

- (1) For the combustion characteristics, the maximum pressure and the maximum heat release rate (HRR) in the cylinder are increased with increase in engine load, but the brake specific fuel consumption (BSFC) is significantly reduced; the addition of ethanol has no significant difference in the variation of maximum in-cylinder pressure, but it respectively increases the maximum HRR and BSFC by 12.95% and 3.98% on average.
- (2) For the emission characteristics, overall, as the load increases, carbon monoxide (CO) emissions of all test fuels show a trend of decreasing first and then increasing, hydrocarbon (HC) emissions show a trend of gradually decreasing, while nitrogen oxide (NOx) emissions and smoke opacity both show a trend of gradually increasing. Compared with diesel fuel, the addition of ethanol reduces CO emissions under high load of 120 Nm; the addition of 5 vol.% ethanol with an appropriate amount reduces HC emissions under all loads; the addition of ethanol reduces NOx emissions under 80 Nm and 120 Nm; the addition of 5 vol.% and 10 vol.% ethanol reduces smoke opacity under all loads; on the whole, the effect of adding ethanol on NOx and smoke emissions reduction is the most obvious at 80 Nm and 120 Nm, respectively, with an average reduction of 5.67% and 36.08% respectively.

The most exciting result in this study is that the addition of ethanol can simultaneously reduce NO_x and smoke emissions under medium and high load conditions. Therefore, the effect of ethanol addition on NO_x emissions reduction will be compared with the operation of exhaust gas recirculation (EGR) in future work.

Author Contributions: Conceptualization, J.C.G.; methodology, J.C.G., J.Y.K. and B.O.Y.; software, J.C.G.; validation, J.C.G. and J.H.S.; formal analysis, J.C.G. and J.H.S.; investigation, J.C.G., J.Y.K., B.O.Y., and J.H.S.; resources, J.C.G., J.Y.K. and B.O.Y.; data curation, J.C.G.; writing—original draft preparation, J.C.G.; writing—review and editing, J.C.G. and J.H.S.; All authors have read and agreed to the published version of the manuscript.

Funding: This research received no external funding.

Institutional Review Board Statement: Not applicable.

Informed Consent Statement: Not applicable.

Data Availability Statement: The data used to support this study are included within the article.

Conflicts of Interest: The authors declare no conflict of interest.

Abbreviations

ATDC: after top dead center; TDC: top dead center; NO_x: nitrogen oxides; EV: electric vehicles; CO₂: carbon dioxide; LCA: life cycle assessment; IEA: International Energy Agency; ICE: Internal Combustion Engine; DOC: diesel oxidation catalyst; VVT: variable valve timing; VCR: variable compression ratio; DPF: diesel particulate filter; BSFC: brake specific fuel consumption; SCR: selective catalytic reduction; EGR: exhaust gas recirculation; CRDI: common rail direct injection; D100: neat diesel fuel; D95E5B1: diesel fuel and ethanol are mixed at a volume ratio of 95:5, and then mixed with 1% biodiesel; D90E10B1: diesel fuel and ethanol are mixed at a volume ratio of 90:10, and then mixed with 1% biodiesel; D85E15B1: diesel fuel and ethanol are mixed at a volume ratio of 85:15, and then mixed with 1% biodiesel; BTDC: before top dead center; BDC: bottom dead center; HRR: heat release rate; SOC: start of combustion.

References

1. Liu, H.; Wang, Z.; Wang, J.; He, X. Improvement of emission characteristics and thermal efficiency in diesel engines by fueling gasoline/diesel/PODEn blends. *Energy* **2016**, *97*, 105–112. [[CrossRef](#)]
2. Xu, G.; Jia, M.; Li, Y.; Chang, Y.; Liu, H.; Wang, T. Evaluation of variable compression ratio (VCR) and variable valve timing (VVT) strategies in a heavy-duty diesel engine with reactivity controlled compression ignition (RCCI) combustion under a wide load range. *Fuel* **2019**, *253*, 114–128. [[CrossRef](#)]
3. Basaran, H.U.; Ozsoysal, O.A. Effects of application of variable valve timing on the exhaust gas temperature improvement in a low-loaded diesel engine. *Appl. Therm. Eng.* **2017**, *122*, 758–767. [[CrossRef](#)]
4. Honardar, S.; Busch, H.; Schnorbus, T.; Severin, C.; Kolbeck, A.F.; Korfer, T. *Exhaust Temperature Management for Diesel Engines Assessment of Engine Concepts and Calibration Strategies with Regard to Fuel Penalty*; SAE Technical Paper; SAE International: Warrendale, PA, USA, 2011.
5. Zhang, Z.; Ye, J.; Tan, D.; Feng, Z.; Luo, J.; Tan, Y.; Huang, Y. The effects of Fe₂O₃ based DOC and SCR catalyst on the combustion and emission characteristics of a diesel engine fueled with biodiesel. *Fuel* **2021**, *290*, 120039. [[CrossRef](#)]
6. Meng, Z.; Chen, C.; Li, J.; Fang, J.; Tan, J.; Qin, Y.; Jiang, Y.; Qin, Z.; Bai, W.; Liang, K. Particle emission characteristics of DPF regeneration from DPF regeneration bench and diesel engine bench measurements. *Fuel* **2020**, *262*, 116589. [[CrossRef](#)]
7. Ko, J.; Si, W.; Jin, D.; Myung, C.-L.; Park, S. Effect of active regeneration on time-resolved characteristics of gaseous emissions and size-resolved particle emissions from light-duty diesel engine. *J. Aerosol Sci.* **2016**, *91*, 62–77. [[CrossRef](#)]
8. Bai, S.; Tang, J.; Wang, G.; Li, G. Soot loading estimation model and passive regeneration characteristics of DPF system for heavy-duty engine. *Appl. Therm. Eng.* **2016**, *100*, 1292–1298. [[CrossRef](#)]
9. Guan, B.; Zhan, R.; Lin, H.; Huang, Z. Review of state of the art technologies of selective catalytic reduction of NO_x from diesel engine exhaust. *Appl. Therm. Eng.* **2014**, *66*, 395–414. [[CrossRef](#)]
10. Baik, J.H.; Yim, S.D.; Nam, I.-S.; Mok, Y.S.; Lee, J.-H.; Cho, B.K.; Oh, S.H. Control of NO_x emissions from diesel engine by selective catalytic reduction (SCR) with urea. *Top. Catal.* **2004**, *30*, 37–41. [[CrossRef](#)]
11. Hountalas, D.T.; Mavropoulos, G.C.; Binder, K.B. Effect of exhaust gas recirculation (EGR) temperature for various EGR rates on heavy duty DI diesel engine performance and emissions. *Energy* **2008**, *33*, 272–283. [[CrossRef](#)]

12. Elkelawy, M.; Alm-Eldin Bastawissi, H.; Esmaeil, K.K.; Radwan, A.M.; Panchal, H.; Sadasivuni, K.K.; Ponnamma, D.; Walvekar, R. Experimental studies on the biodiesel production parameters optimization of sunflower and soybean oil mixture and DI engine combustion, performance, and emission analysis fueled with diesel/biodiesel blends. *Fuel* **2019**, *255*, 115791. [[CrossRef](#)]
13. Singh, A.; Sinha, S.; Choudhary, A.K.; Panchal, H.; Elkelawy, M.; Sadasivuni, K.K. Optimization of performance and emission characteristics of CI engine fueled with Jatropha biodiesel produced using a heterogeneous catalyst (CaO). *Fuel* **2020**, *280*, 118611. [[CrossRef](#)]
14. Sekhar, S.C.; Karuppasamy, K.; Vedaraman, N.; Kabeel, A.E.; Sathyamurthy, R.; Elkelawy, M.; Bastawissi, H.A.E. Biodiesel production process optimization from Pithecellobium dulce seed oil: Performance, combustion, and emission analysis on compression ignition engine fuelled with diesel/biodiesel blends. *Energy Convers. Manag.* **2018**, *161*, 141–154. [[CrossRef](#)]
15. Elkelawy, M.; Bastawissi, H.A.-E.; Esmaeil, K.K.; Radwan, A.M.; Panchal, H.; Sadasivuni, K.K.; Suresh, M.; Israr, M. Maximization of biodiesel production from sunflower and soybean oils and prediction of diesel engine performance and emission characteristics through response surface methodology. *Fuel* **2020**, *266*, 117072. [[CrossRef](#)]
16. Elkelawy, M.; Alm-Eldin Bastawissi, H.; El Shenawy, E.A.; Taha, M.; Panchal, H.; Sadasivuni, K.K. Study of performance, combustion, and emissions parameters of DI-diesel engine fueled with algae biodiesel/diesel/n-pentane blends. *Energy Convers. Manag.* **2021**, *10*, 100058. [[CrossRef](#)]
17. An, H.; Yang, W.M.; Chou, S.K.; Chua, K.J. Combustion and emissions characteristics of diesel engine fueled by biodiesel at partial load conditions. *Appl. Energy* **2012**, *99*, 363–371. [[CrossRef](#)]
18. Shahir, N.S.; Masjuki, N.H.; Kalam, M.; Imran, A.; Ashraful, A. Performance and emission assessment of diesel–biodiesel–ethanol/bioethanol blend as a fuel in diesel engines: A review. *Renew. Sustain. Energy Rev.* **2015**, *48*, 62–78. [[CrossRef](#)]
19. Yilmaz, N. Comparative analysis of biodiesel–ethanol–diesel and biodiesel–methanol–diesel blends in a diesel engine. *Energy* **2012**, *40*, 210–213. [[CrossRef](#)]
20. Kwanchareon, P.; Luengnaruemitchai, A.; Jai-In, S. Solubility of a diesel–biodiesel–ethanol blend, its fuel properties, and its emission characteristics from diesel engine. *Fuel* **2007**, *86*, 1053–1061. [[CrossRef](#)]
21. Noorollahi, Y.; Azadbakht, M.; Ghobadian, B. The effect of different diesterol (diesel–biodiesel–ethanol) blends on small air-cooled diesel engine performance and its exhaust gases. *Energy* **2018**, *142*, 196–200. [[CrossRef](#)]
22. Qi, D.; Leick, M.; Liu, Y.; Chia-fon, F.L. Effect of EGR and injection timing on combustion and emission characteristics of split injection strategy DI-diesel engine fueled with biodiesel. *Fuel* **2011**, *90*, 1884–1891. [[CrossRef](#)]
23. Zhuang, J.; Qiao, X.; Bai, J.; Hu, Z. Effect of injection-strategy on combustion, performance and emission characteristics in a DI-diesel engine fueled with diesel from direct coal liquefaction. *Fuel* **2014**, *121*, 141–148. [[CrossRef](#)]
24. Tse, H.; Leung, C.W.; Cheung, C.S. Investigation on the combustion characteristics and particulate emissions from a diesel engine fueled with diesel-biodiesel-ethanol blends. *Energy* **2015**, *83*, 343–350. [[CrossRef](#)]
25. Sittichompoo, S.; Theinnoi, K.; Sawatmongkhon, B.; Wongchang, T.; Iamcheerangkoon, T.; Phugot, S. Promotion effect of hydrogen addition in selective catalytic reduction of nitrogen oxide emissions from diesel engines fuelled with diesel-biodiesel-ethanol blends. *Alex. Eng. J.* **2022**, *61*, 5383–5395. [[CrossRef](#)]
26. Wei, L.; Cheung, C.S.; Ning, Z. Effects of biodiesel-ethanol and biodiesel-butanol blends on the combustion, performance and emissions of a diesel engine. *Energy* **2018**, *155*, 957–970. [[CrossRef](#)]
27. Venu, H.; Raju, V.D.; Lingesan, S.; Elahi, M.; Soudagar, M. Influence of Al₂O₃ nano additives in ternary fuel (diesel-biodiesel-ethanol) blends operated in a single cylinder diesel engine: Performance, combustion and emission characteristics. *Energy* **2021**, *215*, 119091. [[CrossRef](#)]
28. Zhu, L.; Cheung, C.S.; Zhang, W.G.; Huang, Z. Combustion, performance and emission characteristics of a DI diesel engine fueled with ethanol–biodiesel blends. *Fuel* **2011**, *90*, 1743–1750. [[CrossRef](#)]
29. Okcu, M.; Varol, Y.; Altun, Ş.; Firat, M. Effects of isopropanol-butanol-ethanol (IBE) on combustion characteristics of a RCCI engine fueled by biodiesel fuel. *Sustain. Energy Technol. Assess.* **2021**, *47*, 101443. [[CrossRef](#)]
30. Padala, S.; Woo, C.; Kook, S.; Hawkes, E.R. Ethanol utilisation in a diesel engine using dual-fuelling technology. *Fuel* **2013**, *109*, 597–607. [[CrossRef](#)]
31. Mukhtar, N.A.; Hagos, F.Y.; Aziz, A.R.A.; Abdulah, A.A.; Karim, Z.A.A. Combustion characteristics of tri-fuel (diesel-ethanol-biodiesel) emulsion fuels in CI engine with micro-explosion phenomenon attributes. *Fuel* **2022**, *312*, 122933. [[CrossRef](#)]
32. Shirneshan, A.; Bagherzadeh, S.A.; Najafi, G.; Mamat, R.; Mazlan, M. Optimization and investigation the effects of using biodiesel-ethanol blends on the performance and emission characteristics of a diesel engine by genetic algorithm. *Fuel* **2021**, *289*, 119753. [[CrossRef](#)]
33. Tutak, W.; Jamrozik, A.; Pyrc, M.; Sobiepański, M. A comparative study of co-combustion process of diesel-ethanol and biodiesel-ethanol blends in the direct injection diesel engine. *Appl. Therm. Eng.* **2017**, *117*, 155–163. [[CrossRef](#)]
34. Roy, M.M.; Calder, J.; Wang, W.; Mangad, A.; Diniz, F.C.M. Cold start idle emissions from a modern Tier-4 turbo-charged diesel engine fueled with diesel-biodiesel, diesel-biodiesel-ethanol, and diesel-biodiesel-diethyl ether blends. *Appl. Energy* **2016**, *180*, 52–65. [[CrossRef](#)]
35. Sun, J.; Caton, J.A.; Jacobs, T.J. Oxides of nitrogen emissions from biodiesel-fuelled diesel engines. *Prog. Energy Combust. Sci.* **2010**, *36*, 677–695. [[CrossRef](#)]

36. Sathish, T.; Mohanavel, V.; Arunkumar, M.; Rajan, K.; Soudagar, M.E.M.; Mujtaba, M.A.; Salmen, S.H.; Al Obaid, S.; Fayaz, H.; Sivakumar, S. Utilization of *Azadirachta indica* biodiesel, ethanol and diesel blends for diesel engine applications with engine emission profile. *Fuel* **2022**, *319*, 123798. [[CrossRef](#)]
37. Hulwan, D.B.; Joshi, S.V. Performance, emission and combustion characteristic of a multicylinder DI diesel engine running on diesel–ethanol–biodiesel blends of high ethanol content. *Appl. Energy* **2011**, *88*, 5042–5055. [[CrossRef](#)]
38. Gawale, G.R.; Naga Srinivasulu, G. Experimental investigation of ethanol/diesel and ethanol/biodiesel on dual fuel mode HCCI engine for different engine load conditions. *Fuel* **2020**, *263*, 116725. [[CrossRef](#)]

Disclaimer/Publisher’s Note: The statements, opinions and data contained in all publications are solely those of the individual author(s) and contributor(s) and not of MDPI and/or the editor(s). MDPI and/or the editor(s) disclaim responsibility for any injury to people or property resulting from any ideas, methods, instructions or products referred to in the content.